

Article

# Mintaimycins, a Group of Novel Peptide Metabolites from *Micromonospora* sp. C-3509

Xiaomin Hu<sup>1,2</sup>, Ying Wang<sup>1,2</sup>, Chunyan Zhao<sup>1,2</sup>, Shufen Li<sup>1,2</sup>, Xinxin Hu<sup>1,3</sup>, Xuefu You<sup>1,3</sup>, Jiajia Shen<sup>1,2</sup>, Zhen Wang<sup>1,2</sup> , Bin Hong<sup>1,2</sup>, Bingya Jiang<sup>1,2,\*</sup>, Yu Du<sup>1,2,\*</sup> and Linzhuan Wu<sup>1,2,\*</sup>

- <sup>1</sup> NHC Key Laboratory of Biotechnology of Antibiotics, Institute of Medicinal Biotechnology, Chinese Academy of Medical Sciences and Peking Union Medical College, Beijing 100050, China; xiaomin\_0903@163.com (X.H.); wangying@imb.cams.cn (Y.W.); chunyanzhao333@163.com (C.Z.); lisf0229@163.com (S.L.); huxinxin1985@163.com (X.H.); 13311123098@163.com (X.Y.); shenjiajia@imb.pumc.edu.cn (J.S.); wangzhen@imb.pumc.edu.cn (Z.W.); hongbin@imb.pumc.edu.cn (B.H.)
- <sup>2</sup> CAMS Key Laboratory of Synthetic Biology for Drug Innovation, Institute of Medicinal Biotechnology, Chinese Academy of Medical Sciences and Peking Union Medical College, Beijing 100050, China
- <sup>3</sup> Beijing Key Laboratory of Antimicrobial Agents, Institute of Medicinal Biotechnology, Chinese Academy of Medical Sciences and Peking Union Medical College, Beijing 100050, China
- \* Correspondence: jiangbingya@163.com (B.J.); duyuy@imb.pumc.edu.cn (Y.D.); wulinzhuan@imb.pumc.edu.cn (L.W.); Tel.: +86-10-6316-5283 (L.W.); Fax: +86-10-6301-7302 (L.W.)

**Abstract:** A group of peptide metabolites (1–4), designated as mintaimycins, were isolated from *Micromonospora* sp. C-3509. The planar structures of mintaimycins were determined by combination of mass spectrometry, 1D and 2D NMR spectroscopy, and the stereochemistry of mintaimycins were partially resolved by Marfey's or Mosher's method. Mintaimycins featured a central  $\beta$ -methylphenylalanine or phenylalanine linked at its amino group with 5-methyl-2-hexenoic acid, and at its carboxyl group with 5-hydroxy-norleucine or leucine that combined a derivative of hexanoic acid or 4-methylpentanoic acid. Mintaimycin A<sub>1</sub> (1), the principal component, was found to exhibit the biological activity of inducing pre-adipocyte differentiation of 3T3-L1 fibroblast cells at 10.0  $\mu\text{mol/L}$ .

**Keywords:** *Micromonospora*; mintaimycins; pre-adipocyte differentiation



**Citation:** Hu, X.; Wang, Y.; Zhao, C.; Li, S.; Hu, X.; You, X.; Shen, J.; Wang, Z.; Hong, B.; Jiang, B.; et al.

Mintaimycins, a Group of Novel Peptide Metabolites from *Micromonospora* sp. C-3509. *Molecules* **2022**, *27*, 1150. <https://doi.org/10.3390/molecules27041150>

Academic Editor: Josphat Matasyoh

Received: 27 December 2021

Accepted: 1 February 2022

Published: 9 February 2022

**Publisher's Note:** MDPI stays neutral with regard to jurisdictional claims in published maps and institutional affiliations.



**Copyright:** © 2022 by the authors. Licensee MDPI, Basel, Switzerland. This article is an open access article distributed under the terms and conditions of the Creative Commons Attribution (CC BY) license (<https://creativecommons.org/licenses/by/4.0/>).

## 1. Introduction

*Micromonospora*, a genus of actinomycetes, is most famous for producing secondary metabolites of aminocyclitols with strong antibacterial activity and enediynes with severe antitumor activity. *Micromonospora echinospora* subsp. *calichensis*, for example, is the producer of the clinical antibiotic gentamicin and payload in antibody-drug conjugate calicheamicin [1]. *Micromonospora* is also known for producing secondary metabolites with diverse chemical structures and biological activities. Many bioactive polyene macrolactams, aromatic polyketides and peptides have been identified from the genus [2–8].

We are interested in new secondary metabolites from actinomycetes [9–11]. *Micromonospora* sp. C-3509 as a soil strain isolated from Sheshan in Wuhan of China was previously identified as a calicheamicin producer [12]. To explore whether the strain produced any other secondary metabolites, we performed a microbial chemistry investigation for it. Herein, the discovery of a group of novel peptide metabolites (mintaimycins) from the strain was described.

## 2. Results and Discussion

### 2.1. Discovery of New Secondary Metabolites (Mintaimycins) from *Micromonospora* sp. C-3509

Two HPLC peaks with identical UV absorption profile ( $\lambda_{\text{max}}$  at 208 nm) appeared in the ethyl acetate (EtOAc) extract of *Micromonospora* sp. C-3509 cultured on solid state

fermentation medium. They displayed molecular mass of 500 and 486 amu, respectively, by mass spectrometry (Figures S1–S3). As calicheamicin, with a molecular mass of 1367 amu, was the only reported secondary metabolite of *Micromonospora* sp. C-3509, compounds in these peaks aroused our interest.

An enlarged culture of *Micromonospora* sp. C-3509 was prepared and extracted with EtOAc for isolation and purification of the interested compound(s) (Figure S4). The EtOAc extract was loaded on an ODS column for fractionation. Eluents containing the interested compound(s) were applied on reverse-phase HPLC column for the final isolation and refinement of the interested compound(s) (Figures S5–S8). In the end, four pure compounds 1–4 were obtained (Figures S9–S16).

## 2.2. Structural Elucidation of Mintaimycins (1–4)

Compound **1** was a white amorphous powder. Its molecular formula was deduced as  $C_{29}H_{44}N_2O_5$  by HRESIMS, implying 9 degrees of unsaturation. The  $^1H$  NMR spectrum of **1** displayed resonances attributable to: (a) a di-substituted trans-double bond attached to an aliphatic methylene unit ( $\delta_H$  5.76 (dt,  $J = 15.6, 1.2$  Hz, H-2'), 6.62 (dt,  $J = 15.0, 7.8$  Hz, H-3')), (b) a monosubstituted benzene ring ( $\delta_H$  7.22 (1H, m, H-7),  $\delta_H$  7.27 (2H, m, H-6 and H-8), and  $\delta_H$  7.29 (2H, m, H-5 and H-9)), and (c) six secondary methyls ( $\delta_H$  0.86–1.29, doublets, H-10/H-6'/H-7'/H-1''/H-10''/H-11''). The  $^1H$  NMR spectrum (Figure S17) also displayed four  $sp^3$ -hybridized methylenes, eight  $sp^3$ -hybridized methines and three exchangeable resonances assignable to two amide protons at  $\delta_H$  7.09 (d,  $J = 8.4$  Hz, NH-2) and 7.22 (d,  $J = 10.2$  Hz, NH-1) and a secondary hydroxy proton at  $\delta_H$  4.16 (ddd,  $J = 8.4, 6.0, 1.8$  Hz, H-6''). The  $^{13}C$  NMR and DEPT spectra (Figures S18 and S19) of **1** showed 29 carbon resonances, which corresponded to the above groups and three additional carbonyl carbons ( $\delta_C$  166.4 (C-1'), 172.5 (C-1) and 173.8 (C-12'')).

The planar structure of **1** was resolved by a comprehensive analysis of 2D NMR spectra ( $^1H$ - $^1H$  COSY, HSQC, and HMBC, Figures S20–S22). In the  $^1H$ - $^1H$  COSY spectrum (Figure S20) of **1**, the homonuclear coupling correlations of NH-2/H-2/H-3/H<sub>3</sub>-10 revealed the presence of structural units containing the vicinal coupled protons (Figure 1, thick lines). In the HMBC spectrum of **1**, two- and three-bond correlations of H<sub>3</sub>-10/C-4 ( $\delta_C$  145.2) and C-2, H-3/C-5 ( $\delta_C$  129.2) and C-1 ( $\delta_C$  172.5) were observed. These correlations, in combination with the shifts of these proton and carbon resonances, demonstrated the presence of a  $\beta$ -methylphenylalanine ( $\beta$ -MePhe) unit in **1** (fragment 1 in Figure 1). The  $^1H$ - $^1H$  COSY correlations of H<sub>3</sub>-7'/H-5', H<sub>3</sub>-6'/H-5'/H-4'/H-3'/H-2', and HMBC correlations of H<sub>3</sub>-6'/C-5' and H<sub>2</sub>-4', H<sub>3</sub>-7'/C-5' and C-4', H<sub>2</sub>-4'/C-3' and C-2', and H-3'/C-1', together with the chemical shift of these carbons, indicated the presence of a 5-methyl-2-hexenoic acid unit in **1** (fragment 2 in Figure 1). Meanwhile, the  $^1H$ - $^1H$  COSY correlations of NH-7''/H-7'', H<sub>3</sub>-1''/H-2''/H<sub>2</sub>-3''/H<sub>2</sub>-4''/H-5''/H-6''/H-7''/H<sub>2</sub>-8''/H-9''/H<sub>3</sub>-10'', H<sub>3</sub>-11''/H-9'', the HMBC correlations of H-6'' and H<sub>2</sub>-4''/C-12'', H<sub>3</sub>-11'' and H<sub>3</sub>-10''/C-8'' and together with molecular formula revealed the presence of 3(2-amino-1-hydroxy-4-methylpentyl)-6-methyltetrahydropyranone unit in **1** (fragment 3 in Figure 1, containing a  $\delta$ -lactone ring).

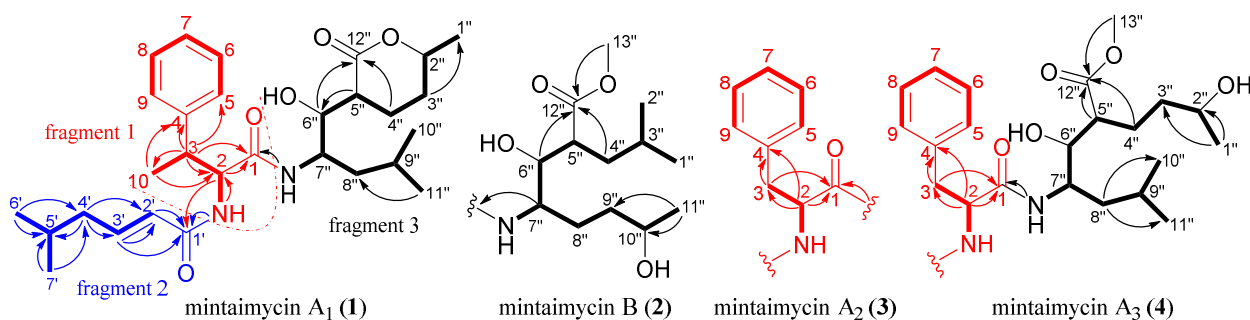


**Figure 1.** The  $^1H$ - $^1H$  COSY (thick lines) and main HMBC (arrows) correlations of mintaimycins A<sub>1–3</sub> and B (1–4).

The connectivity of fragments 1 and 2 via a nitrogen atom (*N*-2) was clearly demonstrated by the HMBC correlation from *NH*-2 to *C*-1' (Figure 1). The association of fragments 1 and 3 via *C*-1-*N* (*NH*-7'') was suggested by the HMBC correlations from *NH*-7'' to *C*-1. Therefore, the planar structure of **1** was determined as in Figure 1, which was further supported by the molecular formula of **1**. A SciFinder search confirmed that **1** was a new compound. Compound **1** as the principal component of **1–4** was designated as mintaimycin A<sub>1</sub>. Its NMR data were assigned in Table 1.

**Table 1.** NMR data of mintaimycins A<sub>1</sub> (1), B (2), A<sub>2</sub> (3) and A<sub>3</sub> (4).

Position	Mintaimycin A <sub>1</sub> (1)		Mintaimycin B (2)		Mintaimycin A <sub>2</sub> (3)		Mintaimycin A <sub>3</sub> (4)	
	$\delta_C$ , Type	$\delta_H$ (J in Hz)	$\delta_C$ , Type	$\delta_H$ (J in Hz)	$\delta_C$ , Type	$\delta_H$ (J in Hz)	$\delta_C$ , Type	$\delta_H$ (J in Hz)
1	172.5, C		170.7, C		171.0, C		172.5, C	
1-NH		7.22, d (10.2)		6.15, d (8.0)		7.88, d (9.6)		7.12, d (8.8)
2	60.8, CH	4.50, dd (10.2, 8.4)	59.1, CH	4.50, t (7.2)	55.0, CH	4.44, m	56.6, CH	4.67, m
3	42.4, CH	3.19, dq (10.2, 6.6)	40.5, CH	3.43, m	37.5, CH <sub>2</sub>	2.88, dd (15.8, 6.6); 2.80, dd (15.8, 9.0)	39.6, CH <sub>2</sub>	2.93, dd (11.9, 7.2); 3.10, dd (11.9, 7.2)
4	145.2, C		141.7, C		137.9, C		139.3, C	
5	129.2, CH	7.29, overlap	127.6, CH	7.24, overlap	128.2, CH	7.25, overlap	130.8, CH	7.26, overlap
6	129.9, CH	7.27, overlap	128.9, CH	7.31, t (7.2)	129.3, CH	7.25, overlap	129.7, CH	7.26, overlap
7	128.0, CH	7.22, m	127.2, CH	7.23, d (7.2)	126.4, CH	7.18, m	127.9, CH	7.19, overlap
8	129.9, CH	7.27, overlap	128.9, CH	7.31, t (7.2)	129.3, CH	7.25, overlap	129.7, CH	7.26, overlap
9	129.2, CH	7.29, overlap	127.6, CH	7.24, overlap	128.2, CH	7.25, overlap	130.8, CH	7.26, overlap
10	20.7, CH <sub>3</sub>	1.29, d (7.2)	18.2, CH <sub>3</sub>	1.30, d (7.2)				
1'	166.4, C		165.8, C		164.9, C		166.5, C	
1'-NH		7.09, d (8.4)		5.77, d (7.2)		8.21, d (8.4)		7.34, d (8.0)
2'	126.5, CH	5.76, dt (15.6, 1.2)	123.7, CH	5.62, d (15.2);	125.4, CH	5.93, d (15.0)	126.7, CH	5.98, d (14.4)
3'	143.9, CH	6.62, td (15.0, 7.8)	145.1, CH	6.70, td (15.2, 7.2)	141.6, CH	6.53, td (15.0, 7.2)	144.0, CH	6.71, dt (14.4, 6.4)
4'	42.4, CH <sub>2</sub>	1.97, m	41.3, CH <sub>2</sub>	2.00, m	40.6, CH <sub>2</sub>	2.00, m	42.5, CH <sub>2</sub>	2.05, overlap
5'	29.3, CH	1.66, m	27.8, CH	1.88, m	27.6, CH	1.67, m	29.3, CH	1.72, m
6'	23.3, CH <sub>3</sub>	0.86, d (6.6)	22.3, CH <sub>3</sub>	0.87, d (6.4)	21.6, CH <sub>3</sub>	0.87, d (6.6)	23.3, CH <sub>3</sub>	0.90, d (6.4)
7'	23.3, CH <sub>3</sub>	0.86, d (6.6)	22.4, CH <sub>3</sub>	0.87, d (6.4)	22.3, CH <sub>3</sub>	0.87, d (6.6)	23.3, CH <sub>3</sub>	0.90, d (6.4)
1''	22.5, CH <sub>3</sub>	1.22, d (6.6)	21.4, CH <sub>3</sub>	0.94, d (6.4)	22.0, CH <sub>3</sub>	1.89, d (6.0)	24.7, CH <sub>3</sub>	1.06, d (6.4)
2''	78.4, CH	4.28, m	23.9, CH <sub>3</sub>	0.93, d (6.4)	76.9, CH	4.27, m	67.3, CH	3.64, overlap
3''	31.7, CH <sub>2</sub>	1.90, m; 1.38, m	24.8, CH	1.64, m	29.8, CH <sub>2</sub>	1.76, m; 1.26, m	38.5, CH <sub>2</sub>	1.37, m; 1.28, m
4''	20.3, CH <sub>2</sub>	1.98, m; 1.89, m	19.5, CH <sub>2</sub>	1.99, m; 1.87, m	18.5, CH <sub>2</sub>	1.83, m; 1.68, m	24.8, CH <sub>2</sub>	1.86, m; 1.72, m
5''	45.3, CH	2.77, ddd (9.0, 7.2, 2.4)	43.8, CH	2.58, m	43.5, CH	2.65, m	49.4, CH	2.51, m
6''	75.3, CH	4.16, ddd (8.4, 6.0, 1.8)	73.8, CH	4.11, overlap	73.0, CH	3.94, ddd (9.0, 6.6, 1.8)	76.2, CH	3.69, m
7''	50.3, CH	4.03, m	49.3, CH	4.10, overlap	48.2, CH	3.64, m	51.3, CH	3.90, m
8''	43.3, CH <sub>2</sub>	1.79, m; 1.38, m	40.8, CH <sub>2</sub>	1.55, m; 1.26, m	41.0, CH <sub>2</sub>	1.46, m; 1.13, m	39.8, CH <sub>2</sub>	1.38, m
9''	26.2, CH	1.79, m	30.3, CH <sub>2</sub>	1.89, m; 1.42, m	24.1, CH	1.14, m	25.5, CH	1.28, m
10''	23.1, CH <sub>3</sub>	0.95, d (6.6)	78.0, CH	4.39, m	22.4, CH <sub>3</sub>	0.74, d (6.6)	22.3, CH <sub>3</sub>	0.78, d (6.4)

Table 1. Cont.

Position	Mintaimycin A <sub>1</sub> (1)		Mintaimycin B (2)		Mintaimycin A <sub>2</sub> (3)		Mintaimycin A <sub>3</sub> (4)	
	$\delta_C$ , Type	$\delta_H$ (J in Hz)	$\delta_C$ , Type	$\delta_H$ (J in Hz)	$\delta_C$ , Type	$\delta_H$ (J in Hz)	$\delta_C$ , Type	$\delta_H$ (J in Hz)
11''	25.2, CH <sub>3</sub>	0.93, d (6.6)	22.0, CH <sub>3</sub>	1.31, d (7.2)	24.2, CH <sub>3</sub>	0.74, d (6.6)	25.1, CH <sub>3</sub>	0.80, d (6.4)
12''	173.8, C		173.8, C		172.9, C		176.2, C	
13''-OCH <sub>3</sub>			50.9, CH <sub>3</sub>	3.49, s			52.2, CH <sub>3</sub>	3.63, s

Note: <sup>1</sup>H and <sup>13</sup>C NMR spectra were measured in acetone-*d*<sub>6</sub> for mintaimycin A<sub>1</sub> (1), CDCl<sub>3</sub> for mintaimycin B (2), DMSO-*d*<sub>6</sub> for mintaimycin A<sub>2</sub> (3), and acetone-*d*<sub>6</sub> for mintaimycin A<sub>3</sub> (4).

Compound **2** was a white amorphous powder. Its molecular formula was deduced by HRESIMS as C<sub>30</sub>H<sub>48</sub>N<sub>2</sub>O<sub>6</sub>, which is CH<sub>3</sub>OH more than **1**. The <sup>1</sup>H and <sup>13</sup>C NMR data (Figures S24 and S25) indicated that **2** was a close homologue of **1**. Analysis of the 2D-NMR data (Figures S26–S30) suggested that **2** should be the  $\delta$ -lactone ring-open (hydrolyzed) and methyl esterified derivative of **1**, and the isobutyl attached at C-7'' and the butyl attached at C-5'' in **1** were exchanged in **2**, which was confirmed by <sup>1</sup>H-<sup>1</sup>H COSY correlations of H<sub>3</sub>-1''/H-3'', and H<sub>3</sub>-2''/H-3''/H<sub>2</sub>-4''/H-5''/H-6''/H-7''/H<sub>2</sub>-8''/H<sub>2</sub>-9''/H-10''/H<sub>3</sub>-11'', HMBC correlations from H-7'' to C-1, H<sub>2</sub>-4'' and H-6'' to C-12'' and OCH<sub>3</sub>-13'' to C-12''. Thus, the planar structure of **2** was depicted as in Figure 1. A SciFinder search indicated that it was the isomer of antibiotic M 9026 factor 3 (Table S1) [13], and they differed only at the *E/Z* configuration of carbon-carbon double bond of fragment 1. Compound **2** was designated as mintaimycin B. Its NMR data were assigned in Table 1.

Compound **3** was a white amorphous powder. Its molecular formula C<sub>28</sub>H<sub>42</sub>N<sub>2</sub>O<sub>5</sub> was determined from the HRESIMS data, which is CH<sub>2</sub> less than **1**. Compound **3** showed nearly identical NMR data to **1** except for the absence of a doublet methyl at  $\delta_C$  20.7 ( $\delta_H$  1.29, d, *J* = 7.2 Hz, C-10), and presence of an additional methene ( $\delta_C$  (37.5, C-3),  $\delta_H$  (2.80, dd, *J* = 15.8, 9.0 Hz; 2.88, dd, *J* = 15.8, 6.6 Hz, H-3)) to replace a methine ( $\delta_C$  (42.4, C-3),  $\delta_H$  (3.19, dq, *J* = 10.2, 6.6 Hz, H-3)) in **1**. Detailed analysis of 1D and 2D NMR data (Figures S31–S37) revealed that **3** was the 3-demethyl derivative of **1**, which was supported by the <sup>1</sup>H-<sup>1</sup>H COSY correlations (Figure 1) of NH-2/H-2/H<sub>2</sub>-3 and the HMBC correlations from NH-1 and H<sub>2</sub>-3 to C-1, and from H-2 and H<sub>2</sub>-3 to C-4. Thus, the planar structure of **3** was depicted as in Figure 1. Compound **3** was designated as mintaimycin A<sub>2</sub>. Its NMR data were assigned in Table 1.

Compound **4** was obtained as a white amorphous powder. Its molecular formula was deduced as C<sub>29</sub>H<sub>46</sub>N<sub>2</sub>O<sub>6</sub> by HRESIMS, which is CH<sub>3</sub>OH more than **3**. Spectroscopic data showed that **4** was a close homologue of **3** except for the signals of a methoxy ( $\delta_C$  52.2,  $\delta_H$  3.63 s, OCH<sub>3</sub>-13'') in **4**. Analysis of 2D-NMR data (Figures S38–S44) suggested that **4** should be the  $\delta$ -lactone ring-open (hydrolyzed) and then methyl esterified derivative of **3**, which was supported by the <sup>1</sup>H-<sup>1</sup>H COSY correlations (Figure 1) of H<sub>2</sub>-4''/H-5''/H-6'' and the HMBC correlations from OCH<sub>3</sub>-13'' to C-12''. Thus, the planar structure of **4** was depicted as in Figure 1. Compound **4** was designated as mintaimycin A<sub>3</sub>. Its NMR data were assigned in Table 1.

### 2.3. Stereochemistry of Mintaimycins

Mintaimycins have five or six chiral carbons for determination of their configurations. The chiral carbon(s) in  $\beta$ -MePhe/Phe of mintaimycins was determined of configuration by Marfey's method [14,15]. Specifically, the  $\beta$ -MePhe in **1–2** was determined as (2*S*, 3*S*)- $\beta$ -MePhe (Figure S45), and the Phe in **3–4** was determined as (2*S*)-Phe (L-Phe, Figures S46 and S47). The chiral carbon C-6'' (with a secondary hydroxy group in **1** and **3**) and C-10'' (with a secondary hydroxy group in **2**) were deduced of their configurations by Mosher's method [16]. Specifically, comprehensive analysis of <sup>1</sup>H NMR resonances of *R*- and *S*-MTPA ester derivatives (Figures S48–S95) revealed systematic distribution of  $\Delta\delta^{SR}$  values ( $\delta^S - \delta^R$  in ppm), thus establishing *R* configuration for chiral carbon C-6'' in **1** and **3** (Figure 2 and Table S2; Table S3 and Figure S96), and *S* configuration for chiral carbon

C-10'' in **2** (Table S4 and Figure S97). According to the plausible pathway proposed for mintaimycins biosynthesis described below, chiral carbon C-6'' in **2** and **4** should take the same configuration as chiral carbon C-6'' in **1** and **3**.

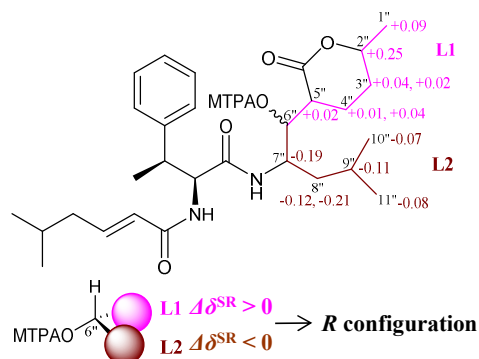


**Figure 2.**  $\Delta\delta^{\text{SR}}$  values measured for the MTPA esters of mintaimycin A<sub>1</sub> (**1**).

There are still chiral carbons C-2'', C-5'' and C-7'' in **1**, **3** and **4**, C-6'' in **4**, and chiral carbons C-5'', C-6'', C-7'' in **2**, undetermined of their configuration(s). So, mintaimycins with partially elucidated stereochemistry were depicted as in Figure 3.

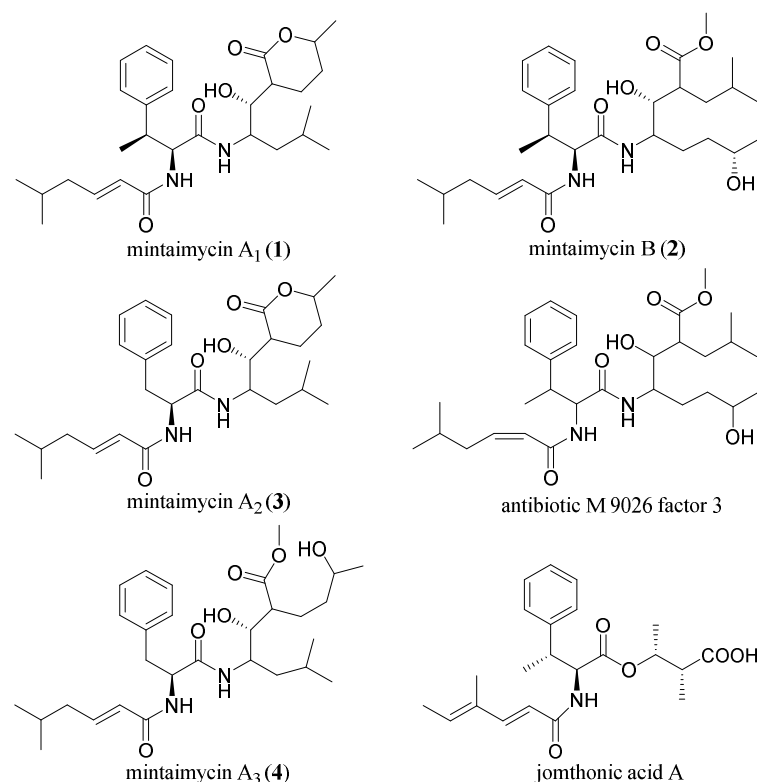


**Figure 3.** Structures of mintaimycins (**1–4**), antibiotic M 9026 factor 3 and jomthonic acid A.

#### 2.4. Speculation of Pathway for Mintaimycins (**1–4**) Biosynthesis

As a group of peptide metabolites with similar or same building/assembling blocks, mintaimycins must have shared the same biosynthetic mechanism. Based on the biosynthetic pathway of jomthonic acids [17], a group of secondary metabolites from *Streptomyces* with similar structure to mintaimycins, a plausible pathway for mintaimycins biosynthesis was proposed as in Figure 4. In the pathway, fragment 1 as the common start building block may come from condensation, keto-reduction, and dehydration of isovaleric acid and acetic acid (catalyzed by polyketide synthase, PKS). Catalyzed by another PKS, fragment 3

may come from condensation and keto-reduction of 5-hydroxy-norleucine or leucine with a derivative of hexanoic acid or 4-methylpentanoic acid (tetrahydro-6-methyl-2*H*-pyran-2-one, methyl 5-hydroxyhexanoate or methyl 4-methylpentanoate). Fragments 1 and 3 are joined with fragment 2 by two amide bonds catalyzed by non-ribosomal peptide synthase (NRPS). Therefore, mintaimycins belong to the biosynthetic products of NRPS-PKS.

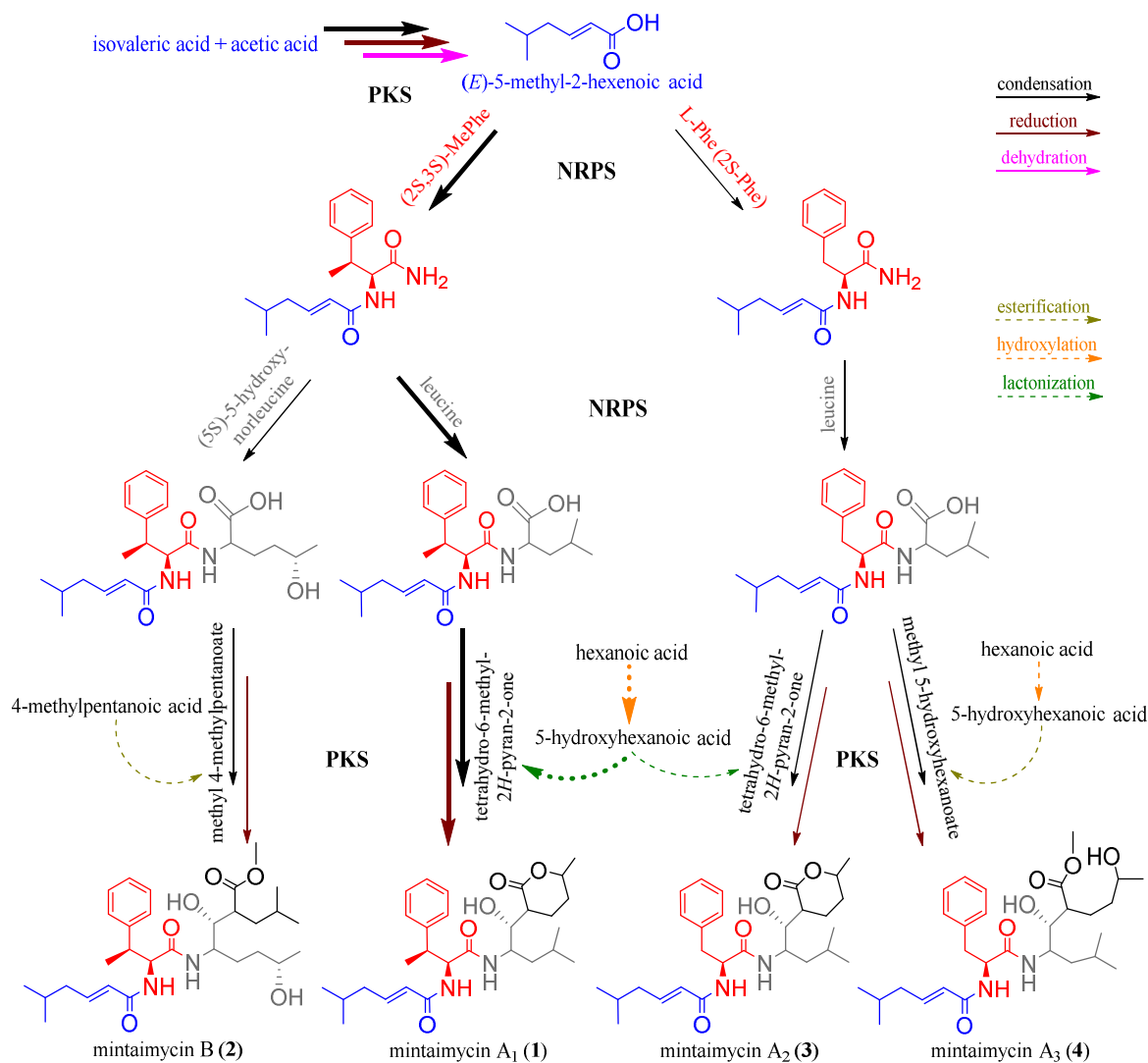


**Figure 4.** The plausible pathway for mintaimycin biosynthesis.

### 2.5. Biological Activities of Mintaimycins

An antibiotic M 9026 complex from *Micromonospora* sp. NRRL 15118 with three antitumor and antimicrobial components was disclosed in the US Patent 4, 692, 333, and planar structure of antibiotic M 9026 factor 3 was provided in SciFinder. As mintaimycins displayed similar structure to antibiotic M 9026 factor 3, we assayed the antibacterial activity of mintaimycins A<sub>1</sub> (1), B (2) and A<sub>2</sub> (3), and cytotoxic activity of mintaimycin A<sub>1</sub> (1). Mintaimycin A<sub>3</sub> (4) was not assayed of its biological activity due to lack of material. Unfortunately, mintaimycins A<sub>1</sub> (1), B (2) and A<sub>2</sub> (3) showed no activity against Gram-positive and -negative bacteria (MIC  $\geq$  32  $\mu$ g/mL, Table S5), and mintaimycin A<sub>1</sub> (1) displayed almost no cytotoxicity against human cell lines HeLa, HGC-27 and PANC-1 (IC<sub>50</sub>  $\geq$  172.98  $\mu$ mol/L, Table S6).

Mintaimycins are also similar to jomthonic acids (a group of secondary metabolites from *Streptomyces*) that possess the biological activity of inducing pre-adipocyte differentiation [14,18]. We assayed mintaimycin A<sub>1</sub> (1) of this activity. At a concentration of



10.0  $\mu\text{mol/L}$ , mintaimycin A<sub>1</sub> (**1**) exhibited a prominent activity of inducing pre-adipocytes to mature adipocytes for 3T3-L1 cells (Figure 5, Figure S98).

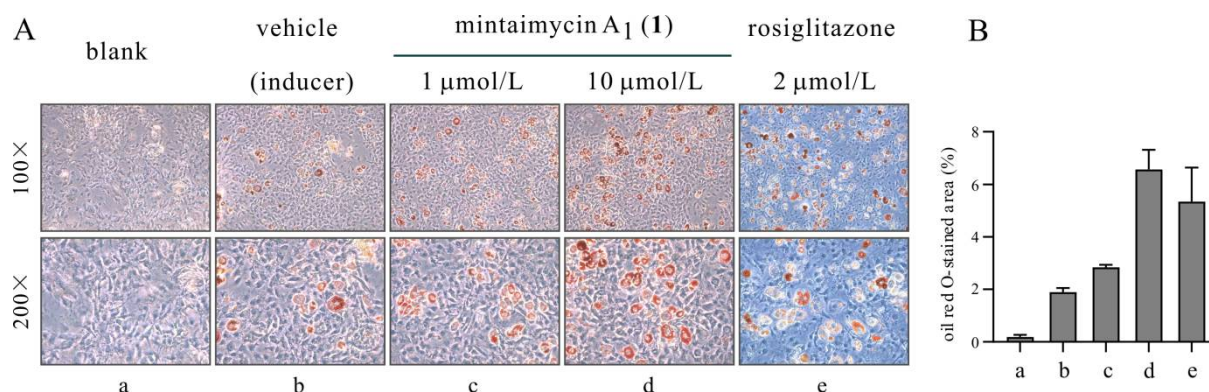


**Figure 5.** Mintaimycin A<sub>1</sub> (**1**) induced differentiation of 3T3-L1 fibroblast cells to adipocytes. Compared to vehicle-treated 3T3-L1 fibroblast cells, cells treated with mintaimycin A<sub>1</sub> (**1**) at 10.0  $\mu\text{mol/L}$  produced prominent oil red O-stained lipid droplets after an incubation period of 14 days, suggesting that it promoted 3T3-L1 fibroblast cells to differentiate into lipid-accumulating adipocytes. Rosiglitazone (an anti-diabetic drug) at 2.0  $\mu\text{mol/L}$  was used as positive control in the assay. A mixture of 10.0  $\mu\text{g/mL}$  of insulin, 0.5  $\text{mmol/L}$  of 3-isobutyl-1-methylxanthine and 1.0  $\mu\text{mol/L}$  of dexamethasone was used as an inducer for cell adipogenesis. (A) Representative images of oil red O staining of 3T3-L1 cells at day 14, a: blank; b: vehicle (inducer); c: 1.0  $\mu\text{mol/L}$  (**1**); d: 10.0  $\mu\text{mol/L}$  (**1**); e: 2.0  $\mu\text{mol/L}$  (rosiglitazone); (B) differentiation-inducing activity quantified by oil red O-stained images (100 $\times$  magnification).

### 3. Materials and Methods

#### 3.1. General Procedures

UV spectra were acquired with a Cary 300 spectrometer. IR spectra were obtained using a Nicolet 5700FTIR microscope spectrometer. Analytical HPLC was conducted on an Agilent system with a 1260 Quat-Pump and DAD detector. For semi-preparative HPLC, a reverse-phase C<sub>18</sub> column (Spursil 5 $\mu\text{m}$  C<sub>18</sub> column: 250  $\times$  10.0 mm) was used with MeCN-H<sub>2</sub>O as a solvent system. LC-MS was performed on a 1100–6410 Triple Quad from Agilent or an Agilent 1100 LC/MSD with a G1946D single quadrupole mass spectrometer. High-resolution mass spectrometry was carried out on a XEVO G2-XS QToF from Waters. NMR data were collected using a Bruker-600 or an ADVANCE HD 800 MHz and a Bruker Avance III HD 700 MHz spectrometer, where chemical shifts ( $\delta$ ) were reported in ppm and referenced to DMSO-*d*<sub>6</sub> solvent signal ( $\delta_{\text{H}}$  2.49 and  $\delta_{\text{C}}$  39.5), CDCl<sub>3</sub> solvent signal ( $\delta_{\text{H}}$  7.26 and  $\delta_{\text{C}}$  77.0) and acetone-*d*<sub>6</sub> solvent signal ( $\delta_{\text{H}}$  2.04 and  $\delta_{\text{C}}$  206.0). 3T3-L1 fibroblast cell (pre-adipocyte) line was purchased from the Cell Center of the Institute of Basic Medicine, Chinese Academy of Medical Sciences.

#### 3.2. Solid State Fermentation of *Micromonospora* sp. C-3509

Frozen stock spores of *Micromonospora* sp. C-3509 were thawed, inoculated on slant medium (tryptone 0.5%, yeast extract 0.3%, malt extract 1.0%, K<sub>2</sub>HPO<sub>4</sub> 0.1%, KH<sub>2</sub>PO<sub>4</sub> 0.1%, and agar 1.5%, pH 7.0–7.2) and incubated at 28  $^{\circ}\text{C}$  for 10–12 days for spore development. Fresh spores were collected and spread on solid state fermentation medium (sucrose 1.6%, dextrin 2.4%, peptone 0.2%, yeast extract 1.2%, trace element solution 2.0 mL (FeSO<sub>4</sub>·7H<sub>2</sub>O, MnCl<sub>2</sub>·4H<sub>2</sub>O and ZnSO<sub>4</sub>·7H<sub>2</sub>O, each at a concentration of 1.0 mg/mL), KI 0.02% and agar 1.5%, pH 7.0) plates, and incubated at 28  $^{\circ}\text{C}$  for 12 days.

#### 3.3. Extraction and Isolation of Mintaimycins (**1–4**)

Solid state fermentation culture (45 L) of *Micromonospora* sp. C-3509 was extracted with an equal volume of EtOAc three times. The EtOAc extract was concentrated under reduced

pressure at room temperature, which yielded a dark brown residue (25.7 g). The residue was loaded onto a preparative ODS column (Spherical C<sub>18</sub>, 40–60 µm, 61 × 219 mm) and fractionated with a stepwise gradient of MeOH-H<sub>2</sub>O at a constant flow rate of 18 mL/min, which yielded fractions F1-F55.

HPLC analysis indicated that a mixture of mintaimycins A<sub>1</sub> (**1**), B (**2**) and A<sub>2</sub> (**3**) appeared in F39-F42. These fractions were combined and dried (78.0 mg), then applied on a C<sub>18</sub> column for repeated semi-preparative HPLC, which yielded pure preparation of mintaimycins A<sub>1</sub> (**1**, 22.5 mg), B (**2**, 8.5 mg) and A<sub>2</sub> (**3**, 7.5 mg).

HPLC analysis indicated that mintaimycins A<sub>3</sub> (**4**) appeared in F37-F38. These fractions were combined and dried (48.0 mg), then applied on a C<sub>18</sub> column for repeated semi-preparative HPLC, which yielded pure preparation of mintaimycins A<sub>3</sub> (**4**, 0.4 mg).

Mintaimycin A<sub>1</sub> (**1**): white amorphous powder;  $[\alpha]_D^{20}$  −21.88 (c 0.32, MeOH); UV-visible (MeOH)  $\lambda_{\max}$  (log  $\epsilon$ ) 206 (4.51) nm; FTIR  $\nu_{\max}$  3297, 3064, 2958, 2872, 1708, 1652, 1544, 1455, 1384, 1332, 1268, 1215, 1136, 1090, 1036, 981, 942, 885, 761, 701 cm<sup>−1</sup>; <sup>1</sup>H and <sup>13</sup>C NMR data, see Table 1; HRESIMS  $m/z$  501.3318 [M + H]<sup>+</sup> (calcd for C<sub>29</sub>H<sub>45</sub>N<sub>2</sub>O<sub>5</sub>, 501.3328).

Mintaimycin B (**2**): white amorphous powder;  $[\alpha]_D^{20}$  −5.26 (c 0.076, MeOH); UV-visible (MeOH)  $\lambda_{\max}$  (log  $\epsilon$ ) 207 (4.49) nm; FTIR  $\nu_{\max}$  3286, 3064, 2958, 2872, 1736, 1656, 1547, 1454, 1369, 1263, 1212, 1134, 1091, 1058, 981, 886, 761, 701 cm<sup>−1</sup>; <sup>1</sup>H and <sup>13</sup>C NMR data, see Table 1; HRESIMS  $m/z$  533.3591 [M + H]<sup>+</sup> (calcd for C<sub>30</sub>H<sub>49</sub>N<sub>2</sub>O<sub>6</sub>, 533.3590).

Mintaimycin A<sub>2</sub> (**3**): white amorphous powder;  $[\alpha]_D^{20}$  −23.75 (c 0.08, MeOH); UV-visible (MeOH)  $\lambda_{\max}$  (log  $\epsilon$ ) 208 (4.47) nm; FTIR  $\nu_{\max}$  3452, 3311, 3063, 2956, 2871, 1713, 1659, 1631, 1541, 1385, 1264, 1089, 981, 945, 887, 743, 698 cm<sup>−1</sup>; <sup>1</sup>H and <sup>13</sup>C NMR data, see Table 1; HRESIMS  $m/z$  487.3175 [M + H]<sup>+</sup> (calcd for C<sub>28</sub>H<sub>43</sub>N<sub>2</sub>O<sub>5</sub>, 487.3172).

Mintaimycin A<sub>3</sub> (**4**): white amorphous powder;  $[\alpha]_D^{20}$  −40 (c 0.01, MeOH); UV-visible (MeOH)  $\lambda_{\max}$  (log  $\epsilon$ ) 209 (4.27) nm; FTIR  $\nu_{\max}$  3282, 3065, 2958, 2871, 1734, 1656, 1553, 1498, 1455, 1367, 1263, 1210, 1124, 1069, 1030, 984, 917, 827, 746, 700 cm<sup>−1</sup>; <sup>1</sup>H and <sup>13</sup>C NMR data, see Table 1; HRESIMS  $m/z$  519.3447 [M + H]<sup>+</sup> (calcd for C<sub>29</sub>H<sub>47</sub>N<sub>2</sub>O<sub>6</sub>, 519.3434).

### 3.4. Stereochemistry of $\beta$ -Methylphenylalanine ( $\beta$ -MePhe) and Phenylalanine (Phe) Residue in Mintaimycins by Marfey's Method

Mintaimycins A<sub>1</sub> (**1**, 50 µg), B (**2**, 50 µg), A<sub>2</sub> (**3**, 120 µg) and A<sub>3</sub> (**4**, 120 µg) were hydrolyzed in 6 N HCl (200 µL) at 100 °C for 12 h. Each hydrolysate was dried and dissolved in distilled water (60 µL), then 1 mol/L of NaHCO<sub>3</sub> (20 µL) and 1% 1-fluoro-2, 4-dinitrophenyl-5-L-leucinamide (L-FDLA, 25 µL, in acetone) was added, followed by an incubation at 40 °C for 1.5 h. Each L-FDLA derivative solution was neutralized with 1 N of HCl (20 µL), then diluted with MeCN (600 µL) for HPLC analysis.

L-FDLA derivatives of commercial (2*R*,3*R*)- $\beta$ -MePhe, (2*R*,3*S*)- $\beta$ -MePhe, (2*S*,3*S*)- $\beta$ -MePhe, (2*S*,3*R*)- $\beta$ -MePhe, D-Phe and L-Phe were also prepared as described above. An HPLC comparison of L-FDLA derivatives from the hydrolysates of **1–2** with L-FDLA derivatives of commercial (2*R*,3*R*)- $\beta$ -MePhe, (2*R*,3*S*)- $\beta$ -MePhe, (2*S*,3*S*)- $\beta$ -MePhe, (2*S*,3*R*)- $\beta$ -MePhe was conducted to determine the stereochemistry of  $\beta$ -MePhe in mintaimycins A<sub>1</sub> (**1**) and B (**2**). An HPLC comparison of L-FDLA derivatives from the hydrolysates of mintaimycins A<sub>2</sub> (**3**) and A<sub>3</sub> (**4**) with L-FDLA derivatives of commercial D-Phe and L-Phe was performed to determine the stereochemistry of Phe in mintaimycins A<sub>2</sub> (**3**) and A<sub>3</sub> (**4**).

### 3.5. Preparation of (R)- and (S)-MTPA Ester Derivatives of Mintaimycins A<sub>1</sub> (**1**), B (**2**) and A<sub>2</sub> (**3**) by Mosher's Method

To the solutions of **1** (2.0 mg, 0.004 mmol), **2** (1.0 mg, 0.002 mmol) or **3** (1.0 mg, 0.002 mmol) in 200 µL of dry CH<sub>2</sub>Cl<sub>2</sub> were added (S)- or (R)-MTPA-Cl (10 equiv) and DMAP (10 equiv). After stirring at 30 °C for 16 h, the solutions were analyzed by LC-MS for ester derivatives (**1R** and **1S**, **2R** and **2S**, **3R** and **3S**). Then, the reaction solutions were evaporated to dryness, and the residues were applied on analytical HPLC column for purification of these ester derivatives. MTPA derivatives (**1R** and **1S**, **2R** and **2S**, **3R** and **3S**) were dissolved in acetone-*d*<sub>6</sub>, CDCl<sub>3</sub> and DMSO-*d*<sub>6</sub>, respectively, for NMR analysis.



### 3.6. Pre-Adipocyte Differentiation Assay

3T3-L1 fibroblast cells were maintained in high-glucose DMEM medium containing 10% FBS. The cells were cultured in the 12-well plate to reach a confluence state. Two days post-confluency, the assay was initiated by incubating cells with 10% FBS DMEM containing the inducer mixture (0.5 mmol/L of 3-isobutyl-1-methylxanthine, 10.0 µg/mL of insulin, and 1.0 µmol/L of dexamethasone). At the same time, 1.0 and 10.0 µmol/L of mintaimycin A<sub>1</sub> (**1**) were added, and 2.0 µmol/L of rosiglitazone was used as a positive control. After 3 days, the medium with inducer mixture was replaced by DMEM containing insulin (10.0 µg/mL) and incubated for another 2 days, then the medium was changed with high-glucose DMEM in the presence of 10% FBS every 2 days. After 14 days, the cells were processed for oil red O staining according to standardized protocol [19].

**Supplementary Materials:** The Supplementary Materials are available online. Figure S1: HPLC and MS analysis of EtOAc extract of *Micromonospora* sp. C-3509. Figure S2: LC-MS analysis of mintaimycin A<sub>1</sub> (**1**). Figure S3: A MS<sup>2</sup> spectrum of mintaimycin A<sub>1</sub> (**1**). Figure S4: Flow chart for isolation and purification of mintaimycins (**1–4**). Figures S5–S8: UV-visible spectra of mintaimycins (**1–4**). Figures S9–S12: IR spectra of mintaimycins (**1–4**). Figures S13–S16: HRESIMS spectra of mintaimycins (**1–4**). Figure S17: <sup>1</sup>H NMR spectrum (600 MHz) of mintaimycin A<sub>1</sub> (**1**) in acetone-*d*<sub>6</sub>. Figures S18–S19: <sup>13</sup>C NMR spectrum (150 MHz), DEPT spectrum (150 MHz) of mintaimycin A<sub>1</sub> (**1**) in acetone-*d*<sub>6</sub>. Figures S20–S22: <sup>1</sup>H-<sup>1</sup>H COSY spectrum (600 MHz), HSQC spectrum (150 MHz), HMBC spectrum (150 MHz) of mintaimycin A<sub>1</sub> (**1**) in acetone-*d*<sub>6</sub>. Figures S24–S25: <sup>1</sup>H NMR spectrum (800 MHz), <sup>13</sup>C NMR spectrum (200 MHz) of mintaimycin B (**2**) in CDCl<sub>3</sub>. Figures S26–S30: DEPT spectrum (150 MHz), <sup>1</sup>H-<sup>1</sup>H COSY spectrum (800 MHz), HSQC spectrum (200 MHz), HMBC spectrum (200 MHz), ROESY spectrum (800 MHz) of mintaimycin B (**2**) in CDCl<sub>3</sub>. Figures S31–S37: <sup>1</sup>H NMR spectrum (600 MHz), <sup>13</sup>C NMR spectrum (150 MHz), DEPT spectrum (150 MHz), <sup>1</sup>H-<sup>1</sup>H COSY spectrum (600 MHz), HSQC spectrum (150 MHz), HMBC spectrum (150 MHz), ROESY spectrum (600 MHz) of mintaimycin A<sub>2</sub> (**3**) in DMSO-*d*<sub>6</sub>. Figures S38–S44: <sup>1</sup>H NMR spectrum (800 MHz), <sup>13</sup>C NMR spectrum (200 MHz), DEPT spectrum (175 MHz), <sup>1</sup>H-<sup>1</sup>H COSY spectrum (800 MHz), HSQC spectrum (200 MHz), HMBC spectrum (200 MHz), ROESY spectrum (800 MHz) of mintaimycin A<sub>3</sub> (**4**) in acetone-*d*<sub>6</sub>. Figure S45: SIM mode (*m/z* 474.1) of mintaimycin A<sub>1</sub> (**1**) and mintaimycin B (**2**) by Marfey's method. Figure S46: HPLC analysis of mintaimycin A<sub>3-4</sub> (**3-4**) by Marfey's method. Figure S47: LC-MS analysis of mintaimycin A<sub>3-4</sub> (**3-4**) by Marfey's method. Figures S48–S53: LC-MS spectra of (*R*)-MTPA and (*S*)-MTPA esters of mintaimycins (**1–3**). Figures S54–S95: NMR data of (*R*)-MTPA and (*S*)-MTPA esters of mintaimycins (**1–3**). Figure S96:  $\Delta\delta^{\text{SR}}$  values measured for the MTPA esters of mintaimycin A<sub>2</sub> (**3**). Figure S97:  $\Delta\delta^{\text{SR}}$  values measured for the MTPA esters of mintaimycin B (**2**). Figure S98: Viability of 3T3-L1 fibroblast cells treated with various concentrations of mintaimycin A<sub>1</sub> (**1**). Table S1: <sup>1</sup>H NMR data of mintaimycin B (**2**) and the known antibiotic M 9026 factor 3. Table S2: <sup>1</sup>H NMR data in Acetone-*d*<sub>6</sub> for the key protons of mintaimycin A<sub>1</sub> (**1**) and its (*R*)-MTPA and (*S*)-MTPA esters. Table S3: <sup>1</sup>H NMR data in DMSO-*d*<sub>6</sub> for the key protons of mintaimycin A<sub>2</sub> (**3**) and its (*R*)-MTPA and (*S*)-MTPA esters. Table S4: <sup>1</sup>H NMR data in CDCl<sub>3</sub> for the key protons of mintaimycin B (**2**) and its (*R*)-MTPA and (*S*)-MTPA esters. Table S5: MIC of mintaimycin A<sub>1</sub> (**1**), mintaimycin B (**2**) and mintaimycin A<sub>2</sub> (**3**) against Gram-positive and negative bacterial strains. Table S6: IC<sub>50</sub> of mintaimycin A<sub>1</sub> (**1**) against human cell lines.

**Author Contributions:** L.W., Y.D. and B.J. conceived the study. X.H. (Xiaomin Hu), Y.W. and C.Z. performed culture and fermentation; X.H. (Xiaomin Hu) performed chemical analysis and compound isolation; B.J. and S.L. performed NMR structure determination. Y.D. and B.H. performed pre-adipocyte differentiation assay; J.S. and Z.W. performed cytotoxicity assay; X.H. (Xinxin Hu) and X.Y. performed antibacterial assay. X.H. (Xiaomin Hu), B.J. and L.W. wrote the manuscript. All authors have read and agreed to the published version of the manuscript.

**Funding:** This work was supported by National Key Research and Development Program of China (2018YFA0902000), the CAMS Innovation Fund for Medical Sciences (CIFMS, 2021-I2M-1-055) and National Natural Science Foundation of China (81903530).

**Institutional Review Board Statement:** Not applicable.

**Informed Consent Statement:** Not applicable.

**Data Availability Statement:** Not applicable.

**Acknowledgments:** NMR and MS analyses were performed at Nuclear Magnetic Resonance Center of Institute of Materia Medica, CAMS & PUMC.

**Conflicts of Interest:** The authors declare no conflict of interest.

**Sample Availability:** Not available.

## References

1. Maiese, W.M.; Lechevalier, M.P.; Lechevalier, H.A.; Korshalla, J.; Kuck, N.; Fantini, A.; Wildey, M.J.; Thomas, J.; Greenstein, M. Calicheamicins, a novel family of antitumor antibiotics: Taxonomy, fermentation and biological properties. *J. Antibiot.* **1989**, *42*, 558–563. [[CrossRef](#)] [[PubMed](#)]
2. Skellam, E.J.; Stewart, A.K.; Strangman, W.K.; Wright, J.L. Identification of micromonolactam, a new polyene macro cyclic lactam from two *Marine Micromonospora* strains using chemical and molecular methods: Clarification of the biosynthetic pathway from a glutamate starter unit. *J. Antibiot.* **2013**, *66*, 431–441. [[CrossRef](#)] [[PubMed](#)]
3. Nie, Y.L.; Wu, Y.D.; Wang, C.X.; Lin, R.; Xie, Y.; Fang, D.S.; Jiang, H.; Lian, Y.Y. Structure elucidation and antitumour activity of a new macrolactam produced by marine-derived actinomycete *Micromonospora* sp. FIM05328. *Nat. Prod. Res.* **2018**, *32*, 2133–2138. [[CrossRef](#)] [[PubMed](#)]
4. Antal, N.; Fiedler, H.P.; Stackebrandt, E.; Beil, W.; Stroch, K.; Zeeck, A. Retymicin, galtamycin B, saquayamycin Z and ribofuranosyllumichrome, novel secondary metabolites from *Micromonospora* sp. Tü 6368. I. Taxonomy, fermentation, isolation and biological activities. *J. Antibiot.* **2005**, *58*, 95–102. [[CrossRef](#)] [[PubMed](#)]
5. Furumai, T.; Igarashi, Y.; Higuchi, H.; Saito, N.; Oki, T. Kosinostatin, a quinocycline antibiotic with antitumor activity from *Micromonospora* sp. TP-A0468. *J. Antibiot.* **2002**, *55*, 128–133. [[CrossRef](#)] [[PubMed](#)]
6. Pang, X.; Zhao, J.; Fang, X.; Liu, H.; Zhang, Y.; Cen, S.; Yu, L. Surfactin derivatives from *Micromonospora* sp. CPCC 202787 and their anti-HIV activities. *J. Antibiot.* **2017**, *70*, 105–108. [[CrossRef](#)] [[PubMed](#)]
7. McBrien, K.D.; Berry, R.L.; Lowe, S.E.; Neddermann, K.M.; Bursucker, I.; Huang, S.; Klohr, S.E.; Leet, J.E. Rakacidins, new cytotoxic lipopeptides from *Micromonospora* sp. fermentation, isolation and characterization. *J. Antibiot.* **1995**, *48*, 1446–1452. [[CrossRef](#)] [[PubMed](#)]
8. Qi, S.; Gui, M.; Li, H.; Yu, C.; Li, H.; Zeng, Z.; Sun, P. Secondary Metabolites from *Marine Micromonospora*: Chemistry and Bioactivities. *Chem. Biodivers.* **2020**, *17*, e2000024. [[CrossRef](#)]
9. Hu, X.; Hu, X.; Hu, X.; Li, S.; Li, L.; Yu, L.; Liu, H.; You, X.; Wang, Z.; Li, L.; et al. Cytotoxic and Antibacterial Cervinomycins B<sub>1-4</sub> from a *Streptomyces* Species. *J. Nat. Prod.* **2019**, *82*, 2337–2342. [[CrossRef](#)]
10. Li, L.; Li, S.; Jiang, B.; Zhang, M.; Zhang, J.; Yang, B.; Li, L.; Yu, L.; Liu, H.; You, X.; et al. Isarubrolones Containing a Pyridooxazinium Unit from *Streptomyces* as Autophagy Activators. *J. Nat. Prod.* **2019**, *82*, 1149–1154. [[CrossRef](#)] [[PubMed](#)]
11. Wang, J.; Hu, X.; Sun, G.; Li, L.; Jiang, B.; Li, S.; Bai, L.; Liu, H.; Yu, L.; Wu, L. Genome-Guided Discovery of Pretilactam from *Actinosynnema pretiosum* ATCC 31565. *Molecules* **2019**, *24*, 2281. [[CrossRef](#)] [[PubMed](#)]
12. Zhao, C.; Zhang, W.; Gao, R.; Jin, L.; Li, D.; Shao, R. Separation, purification and structure identification of the antitumor antibiotic component from fermentation broth of a new *Micromonospora* sp. C-3509. *Chin. J. New Drugs* **2010**, *19*, 564–568.
13. Pirali, G.; Pagani, H.; Grandi, M.; Paternoster, M.; Tamoni, G.; Cassani, G. Antimicrobial and Antitumor Antibiotic M 9026 and Its Pure Individual Factors 1, 2 and 3, and Microbial Process for Production thereof. U.S. Patent 4692333, 8 September 1987.
14. Igarashi, Y.; Yu, L.; Ikeda, M.; Oikawa, T.; Kitani, S.; Nihira, T.; Bayanmunkh, B.; Panbangred, W. Jomthonic acid, a modified amino acid from a soil-derived *Streptomyces*. *J. Nat. Prod.* **2012**, *75*, 986–990. [[CrossRef](#)] [[PubMed](#)]
15. Jiao, W.H.; Khalil, Z.; Dewapriya, P.; Salim, A.A.; Lin, H.W.; Capon, R.J. Trichodermides A–E: New Peptaibols Isolated from the Australian Termite Nest-Derived Fungus *Trichoderma virens* CMB-TN16. *J. Nat. Prod.* **2018**, *81*, 976–984. [[CrossRef](#)] [[PubMed](#)]
16. Annang, F.; Perez-Victoria, I.; Perez-Moreno, G.; Domingo, E.; Gonzalez, I.; Tormo, J.R.; Martin, J.; Ruiz-Perez, L.M.; Genilloud, O.; Gonzalez-Pacanowska, D.; et al. MDN-0185, an Antiplasmodial Polycyclic Xanthone Isolated from *Micromonospora* sp. CA-256353. *J. Nat. Prod.* **2018**, *81*, 1687–1691. [[CrossRef](#)] [[PubMed](#)]
17. Garcia-Salcedo, R.; Alvarez-Alvarez, R.; Olano, C.; Canedo, L.; Brana, A.F.; Mendez, C.; de la Calle, F.; Salas, J.A. Characterization of the Jomthonic Acids Biosynthesis Pathway and Isolation of Novel Analogues in *Streptomyces caniferus* GUA-06-05-006A. *Mar. Drugs* **2018**, *16*, 259. [[CrossRef](#)] [[PubMed](#)]
18. Yu, L.; Oikawa, T.; Kitani, S.; Nihira, T.; Bayanmunkh, B.; Panbangred, W.; Igarashi, Y. Jomthonic acids B and C, two new modified amino acids from *Streptomyces* sp. *J. Antibiot.* **2014**, *67*, 345–347. [[CrossRef](#)] [[PubMed](#)]
19. Mehlem, A.; Hagberg, C.E.; Muhl, L.; Eriksson, U.; Falkevall, A. Imaging of neutral lipids by oil red O for analyzing the metabolic status in health and disease. *Nat. Protoc.* **2013**, *8*, 1149–1154. [[CrossRef](#)] [[PubMed](#)]